Langmuir

Article

pubs.acs.org/Langmuir

Anticancer Drug-Loaded Gliadin Nanoparticles Induce Apoptosis in Breast Cancer Cells

Muhammad Gulfam,[†] Ji-eun Kim,[†] Jong Min Lee,[†] Boram Ku,[†] Bong Hyun Chung,[‡] and Bong Geun Chung*,[†]

[†]Department of Bionano Engineering, Hanyang University, Ansan, Korea

[‡]BioNanotechnology Research Center, Korea Research Institute of Bioscience and Biotechnology, Daejeon, Korea

ABSTRACT: Nanoscale drug carriers play an important role in regulating the delivery, permeability, and retention of the drugs. Although various carriers have been used to encapsulate anticancer drugs, natural biomaterials are of great benefit for delivery and controlled release of drugs. We used the electrospray deposition system to synthesize gliadin and gliadin-gelatin composite nanoparticles for delivery and controlled release of an anticancer drug (e.g., cyclophosphamide). The size profile and synthesis of nanoparticles was characterized by dynamic light scattering and X-ray diffractometry. Cyclophosphamide was gradually released from the gliadin nanoparticles for 48 h. In contrast, the gliadin-gelatin composite nanoparticles released cyclophosphamide in a rapid manner. Furthermore, we demonstrated that breast cancer cells cultured with cyclophosphamide-loaded 7% gliadin nanoparticles for 24 h became apoptotic, confirmed by Western blotting analysis. Therefore, the gliadin-based nanoparticle could be a powerful tool for delivery and controlled release of anticancer drugs.

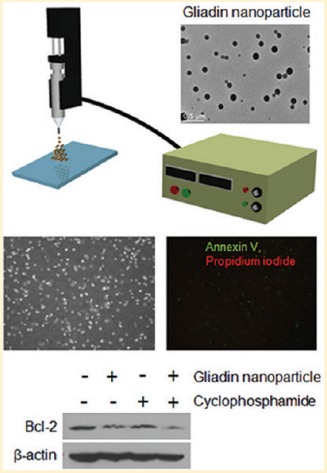

INTRODUCTION

Drug carriers play an important role in controlling the nonspecific toxicity of free drugs, which are poorly soluble and instable. To reduce nonspecific toxicity, anticancer drugs can be loaded into a nanoparticle that delivers the drug into malignant cells.[1] Various types of therapeutic agents (e.g., cyclophosphamide, doxorubicin, paclitaxel, and cisplatin) have been used in cancer therapy. Cyclophosphamide, a cyclic phosphamide ester of mechlorethamine, cross-links DNA and prevents cell division.[2] Cyclophosphamide has been used to treat retinoblastoma, neuroblastoma, lung cancer, and breast cancer.[3−5] Although cyclophosphamide is effective for cancer therapy, it damages the tissues.[6−8] To overcome this problem, cyclophosphamide has been loaded within carriers, which safely deliver the drug to the target. Butylcyanoacrylate spheres containing cyclophosphamide have been used to treat ocular inflammation in the inner cavity of the eye.[9,10] It demonstrated that cyclophosphamide was incorporated in butylcyanoacrylate spheres for ocular drug delivery, showing the treatment of severe ocular inflammation without any corneal irritation. Rat gliomas have also been treated using cyclophosphamide-loaded biodegradable polymers.[11] *In vitro* study demonstrated the effect of cyclophosphamide-loaded polymers on treating medulloblastoma cells, showing that the tumor was reduced by cyclophosphamide-loaded polymers.

In the past few decades, various drug-loaded carriers (e.g., micelle, liposome, and polymer−drug conjugate) have been developed to enhance tumor targeting, drug delivery, and controlled release.[12−14] In particular, polymeric particles are of great interest in targeting the tumors for cancer therapy applications.[15,16] Natural polymers (e.g., polysaccharides, polypeptides, and lipids) are less toxic and safer than synthetic polymers.[17,18] In addition, natural polymers are promising carriers for delivery and controlled release of drugs, because they are biodegradable, nontoxic, and stable.[19,20] The hydrogel nanoparticles have also been used to analyze their drug delivery potential. The hydrogels, which are water-soluble polymers,[21] are of great interest in drug delivery applications. Various hydrogel-based nanoparticles have recently been developed using natural and synthetic polymers. The natural polymers (e.g., chitosan, alginate, and gelatin) have extensively been used to create hydrogel nanoparticles. The synthetic polymers (e.g., poly(vinyl alcohol), poly(ethylene oxide), poly(ethyleneimine), poly(vinyl pyrrolidone), and poly-*N*-isopropylacrylamide) have been employed for drug delivery applications.[22] The porosity of hydrogels enabled the control of the drug loading into the gel matrix and released the drug in a temporal and spatial manner.[23] In particular, the polymeric implants of gelatin cross-linked with glutaraldehyde have previously been investigated to demonstrate safety and biocompatibility.[24−28] For instance, the pro-angiogenic characteristics of a cross-linked gelatin matrix have been examined.[26] The cross-linked gelatin

Received: February 16, 2012
Revised: May 8, 2012
Published: May 8, 2012

sponge stimulated the blood vessel formation (e.g., angiogenesis) without the release of toxic components. Implantation of gelatin sponges onto the chorioallantoic membrane of fertilized chicken eggs induced robust attraction of endothelial cells and formation of blood vessels. The three-dimensional (3D) gelatin hydrogel structures have been used to repair traumatic brain injury.[27] 3D gelatin hydrogel structures were implanted into cortical defects in rat brains, showing good biocompatibility in brain tissue repairs. Furthermore, the gelatin and gelatin/chitosan implants have been used in rat liver tissues.[28] It demonstrated that the gelatin gel showed a faster biodegradation rate and relatively low antigenic response. It was also revealed that the gelatin/chitosan gel induced fibrin formation and vascularization at the implant−host interface.

In general, conventional drug delivery methods (e.g., oral or intravenous delivery) have limitations to deliver anticancer drugs to the target.[29] Furthermore, the acidic environment of the alimentary tract rapidly degrades anticancer drugs. To overcome these limitations, it is important to engineer a drug delivery system that can tolerate the acidic environment. The gliadin, a natural glycoprotein, can adhere to the mucus layer of the stomach due to its mucoadhesive property, which is a result of various interactions (e.g., hydrogen bonding, van der Waals force, and mechanical penetration).[30] Gliadin contains neutral amino acids, which enhance hydrogen bonding with the mucus layer, and lipophilic amino acids that support hydrophilic interactions.[31,32] Furthermore, the gliadin, a plant protein, does not contain prions,[33] which are misfolded proteins found in animals.[34] Gliadin particles have previously been generated for drug delivery and controlled release applications. For example, gliadin particles have been used to control the release of retinoic acid.[35] The gliadin particles had low solubility in water due to their hydrophobicity and were highly stable in buffer solution. The stability of gliadin nanoparticles increased when chemically cross-linked with glutaraldehyde. The gliadin particles containing amoxicillin have also been created to treat *Helicobacter pylori*.[29] Gliadin particles containing amoxicillin were synthesized by desolvation method. The mucoadhesion of the gliadin particles increased with gliadin concentrations. Although various drugs have been loaded into gliadin particles for delivery and controlled release, gliadin nanoparticles loaded with anticancer drugs have not yet been fully explored.

To generate polymeric particles, various methods (e.g., desolvation, emulsification, precipitation, and electrospray deposition) have been used.[31,36,37] Although the gliadin particle can be synthesized using the desolvation method,[31,35,36,38] it has some limitations, such as low drug loading efficiency and inability to separate particles from the aqueous phase.[39] The electrospray deposition system, which uses liquid atomization by means of electrical forces, has several advantages over conventional methods, such as high drug loading efficiency and self-dispersion. Furthermore, nanoparticles synthesized by electrospray deposition systems do not require any template or surfactant.[40] The electrosprayed gliadin nanoparticles enabled the physical entrapment of the drug, showing that cyclophosphamide could disperse in the polymeric matrix of nanoparticles, as previously described.[10] The lipophilic amino acid, one of the components in gliadin protein, bound to cyclophosphamide due to hydrophilic interactions. As a result, the gliadin-based nanoparticles could bind to a cyclophosphamide anticancer drug, as previously described.[29] Here, we created gliadin-based nanoparticles loaded with cyclophosphamide using an electrospray deposition system. The gliadin-based nanoparticles controlled the release of an anticancer drug to induce apoptosis in breast cancer cells. Therefore, gliadin-based nanoparticles could be useful for regulating the delivery and release of anticancer drugs in a controlled manner.

MATERIALS AND METHODS

Gliadin Extraction and Purification. Gluten was extracted from wheat flour, freeze−dried, ground in an electrical grinder, and defatted by two extractions with dichloromethane for 2 h at 20 °C (gluten/solvent ratio: 1/10). After filtration, the residual solvent was evaporated from the gluten at 20 °C. Samples of dried gluten powder (100 g) were gently stirred in an ethanol/water mixture (70/30 v/v; gluten/solvent ratio: 1/10) for 4 h at 20 °C. The suspension was centrifuged at 4600 rpm. The soluble fraction, primarily gliadin with some glutenin proteins, was freeze−dried again. To completely remove the glutenins, the freeze−dried gliadin was washed with distilled water. After filtering, it was treated with 0.05 M acetic acid and freeze−dried.

Synthesis of Gliadin or Gliadin−Gelatin Composite Nanoparticles. To synthesize gliadin nanoparticles, 7% gliadin was dissolved in 70% ethanol. The solution was stirred at room temperature for 2 h and then aged for 2 days. After filtering, gliadin nanoparticles were synthesized using electrospray deposition system (Figure 1A). The electrospray deposition system consisted of a syringe pump (Nano NC, Korea), high-voltage supply, and grounded collector. The gliadin polymer solution was loaded in a 10 mL syringe and continuously infused using the syringe pump (flow rate of 0.5 mL/h) and a stainless steel nozzle with a diameter of 32 GA, which was connected to the high-voltage power supply. The high-voltage power supply generated a 12−14 kV potential difference between the nozzle and the ground stainless steel sheet. To generate composite nanoparticles, gelatin was dissolved in 90% acetic acid and gliadin was dissolved in 70% ethanol. The solutions were mixed at a 1:1 ratio. The gliadin−gelatin composite nanoparticles were cross-linked with 2 g glutaraldehyde per 100 g polymer and were subsequently incubated at 25 °C for 60 min. To prepare the cyclophosphamide-loaded gliadin or gliadin−gelatin composite nanoparticles, cyclophosphamide (1 mg cyclophosphamide/1 mL polymer solution) was mixed in the polymer solution and the mixture was subsequently electrosprayed to generate anticancer drug-loaded gliadin or gliadin−gelatin composite nanoparticles.

Morphological Characterization of Nanoparticles. The morphology of gliadin or gliadin−gelatin composite nanoparticles was characterized by scanning electron microscopy (SEM, TESCAN model: VEGA/SBH Motorize). The nanoparticles were coated with platinum (5 wt % on activated carbon) using a turbo sputter coater (EMITECH: K575X/Carb Peltier Cooled). SEM images were obtained at 20 kV. The morphologies of gliadin or gliadin−gelatin composite nanoparticles were confirmed by transmission electron microscopy (TEM, JEM-2100F) at 200 kV, 95 μA dark current, and 126 μA emission current.

Size Profile Distribution and Zeta Potential Measurement. To determine the size profile distribution and zeta potential, nanoparticles were dispersed in deionized water and sonicated using a tip sonicator (Sonics: Vibracell) at 20% amplitude for 3 min. The size profile distribution and zeta potential of nanoparticles were measured with dynamic light scattering using a Zetasizer 4 (Malvern Instruments Ltd., U.K.). To measure the size profile distribution of gliadin or gliadin−gelatin composite nanoparticles, samples were placed in polystyrene cuvettes at 25 °C and 90° angle. The zeta potentials of gliadin or gliadin−gelatin composite nanoparticles were measured by a laser-based multiple angle particle electrophoresis analyzer (Malvern Zetasizer, DTS v 4.10, Malvern Instruments Ltd., U.K.). For zeta potential measurements, the ultrasonicated nanoparticles were placed in the electrophoretic cell with an electric field of 15.24 V/cm.

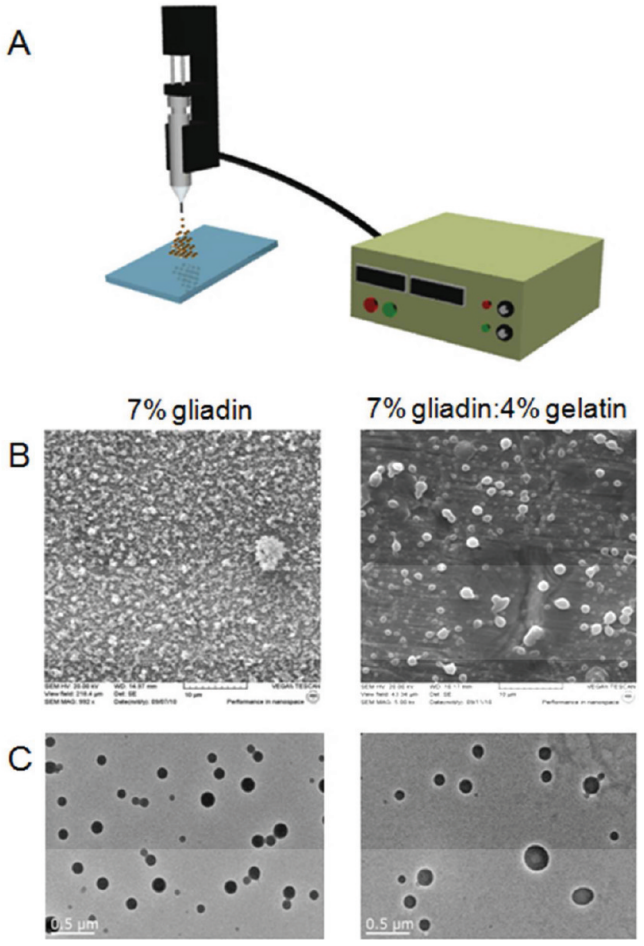

Figure 1. (A) Schematic of the electrospray deposition system to synthesize gliadin-based nanoparticles. (B) Scanning electron microscopy images of nanoparticles produced with 7% gliadin and 7% gliadin/4% gelatin. (C) Transmission electron microscopy images of nanoparticles produced with 7% gliadin and 7% gliadin/4% gelatin.

X-ray Diffraction Analysis. The synthesis of gliadin–gelatin composite nanoparticles was analyzed by X-ray diffractometer (Rigaku Corporation, Japan). A diffracted beam monochromator and a copper target X-ray tube (40 kV, 30 mA) was used to observe the diffraction pattern of gliadin or gliadin–gelatin composite nanoparticles. The diffraction patterns were recorded with 2θ values, ranging from 10° to 40°.

Analysis of Controlled Drug Release. To measure controlled drug release from nanoparticles, nanoparticles were loaded with the anticancer drug, cyclophosphamide. Drug-loaded nanoparticles were dispersed in 100 mL deionized water. Five milliliters of sample was removed from the bulk solution and replaced with 5 mL deionized water to maintain 100 mL volume. The sample was centrifuged at 4600 rpm and the amount of drug in the supernatant was measured. Drug release was measured at 1, 4, 8, 12, 24, and 48 h using a UV–vis spectrophotometer. The calorimetric method, which is based on measuring the nitroso derivative of cyclophosphamide, was used. In a 5 mL sample, 1 mL of 5% hydrochloric acid was added to 1 mL of 20% sodium nitrite and heated in a 65 °C water bath for 20 min. The solution was then cooled and 5 mL of 15% sulfamic acid was added under vigorous stirring. The solution was cooled again and 2 mL of 20% sodium hydroxide was added. After adding the sodium hydroxide, the resulting solution was diluted with deionized water to maintain 20 mL volume. The cyclophosphamide concentration was calculated from a calibration curve (20–80 μg/mL) at 325 nm using a UV–vis spectrophotometer. To calculate the total drug loading in gliadin-based nanoparticles, the cyclophosphamide-loaded nanoparticles were dispersed in 70% ethyl alcohol and were subsequently stirred for 24 h. The suspension was centrifuged at 4600 rpm for 10 min, and the supernatant was analyzed to measure the drug amount. As gliadin is soluble in 70% ethyl alcohol, gliadin polymer was dissolved in 70% ethyl alcohol to release the cyclophosphamide. The drug release experiments were performed three times. All data were presented as means ± standard deviations and were statistically compared using Student's t test. p-values less than 0.05 or 0.01 were considered statistically significant. All error bars illustrated standard deviations. The drug release from 7% gliadin/8% gelatin composite nanoparticles was statistically compared to the drug released from 7% gliadin and 7% gliadin/4% gelatin composite nanoparticles.

Breast Cancer Cell Culture and Apoptosis Assay. MCF7 breast cancer cells were cultured with Dulbecco's Modified Eagle Medium (DMEM) containing 10% fetal bovine serum (FBS). Cell culture medium was changed every 2 days. An apoptosis assay (Invitrogen, USA) was used to determine the apoptotic cells (stained by Annexin V, green) and necrotic cells (stained by propidium iodide, red).

Western Blot Analysis. MCF7 cells were treated with 3.5 mg gliadin nanoparticles loaded with 3.5 mM cyclophosphamide. Harvested cells were disrupted in cell lysis buffer (0.02 M Tris–HCl pH 7.4, 1% Triton X-100, 150 mM NaCl, 1 mM EDTA, 1 mM EGTA, 1 mM phenylmethylsulfonyl fluoride, 0.25 M sucrose, protease, 0.5% sodium deoxycholate, and phosphatase inhibitor cocktail (Roche, USA)) for 30 min on ice. The homogenates were sonicated for 30 s on ice and centrifuged at 13 000 rpm for 10 min at 4 °C. Total protein concentration in the extracts was determined using Bradford reagent (Sigma, USA). Equal amounts of protein (50 μg) were resolved by 15% SDS-polyacrylamide gel electrophoresis and then transferred to nitrocellulose membrane (Pall Corporation, USA). The membranes were soaked in blocking buffer (5% skim milk in phosphate buffered saline) for 1 h at room temperature and incubated overnight with primary antibodies, such as Bcl-2 (Santa Cruz, USA) and β-actin (Sigma, USA). Immunoreactivity was detected using the chemiluminescence system (AB frontier, Korea).

BrdU Incorporation Assay. Cells were treated with 3.5 mg gliadin nanoparticles loaded with 3.5 mM cyclophosphamide for 12 and 24 h. The cell damage induced by cyclophosphamide-loaded 7% gliadin nanoparticles was analyzed using a BrdU proliferation kit (Roche Molecular Diagnostics, Germany).

RESULTS AND DISCUSSION

Synthesis of Gliadin-Based Nanoparticles. Nanoparticles derived from natural sources are of great benefit for drug delivery, controlled release, and cancer therapy. To synthesize nanoparticles from a natural polymer, we extracted gliadin from wheat flour. Wheat gluten is viscoelastic and has a high tensile strength and excellent gas barrier property.[36] The gliadin was extracted from gluten, which consisted of gliadin, glutenin, albumin, and globulin. Albumin and globulin are water-soluble and can be removed through water extraction. However, gliadin shows higher solubility in 70% ethyl alcohol. We extracted gliadin using 70% ethyl alcohol and removed the glutenin by acetic acid extraction. After extraction of the gliadin from wheat flour, we created gliadin nanoparticles using electrospray deposition system (Figure 1A). The electrospraying system is similar to the electrospinning process. Electrosprayed nanoparticles can be created when the viscosity of the liquid is sufficiently low. It has been known that nanofibrous nonwoven meshes were generated at high concentrations of polymers.[41] In contrast, nanoparticles were created at low concentrations of polymers because the viscosity was proportional to polymer concentrations, as previously described.[42] The electrospray deposition system generated a plume of droplets by charging the liquid at a high voltage. The charged droplets were sprayed from the tip of the nozzle.[40] We generated gliadin-based

dx.doi.org/10.1021/la300691n | Langmuir 2012, 28, 8216–8223

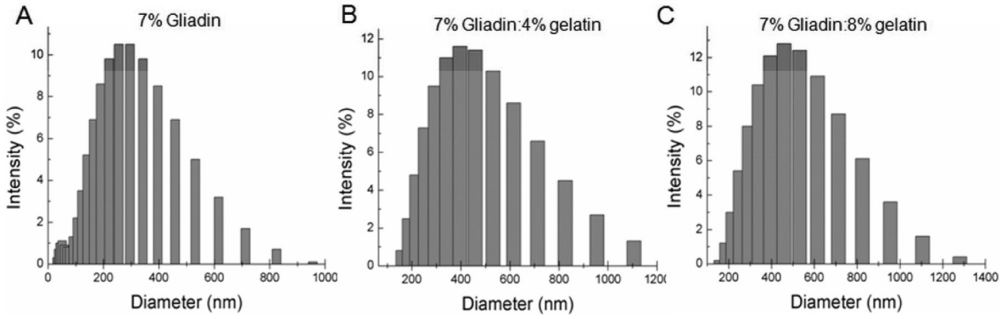

Figure 2. Size profile distribution of nanoparticles using dynamic light scattering: (A) 7% gliadin, (B) 7% gliadin/4% gelatin, and (C) 7% gliadin/8% gelatin.

nanoparticles using 7% gliadin and 4% gelatin concentrations. SEM images showed that the nanoparticles were spherical (Figure 1B). TEM images also showed gliadin-based nanoparticles (7% gliadin, 7% gliadin/4% gelatin) that were homogeneous in shape and size, showing that the size of gliadin–gelatin composite nanoparticles was larger as compared to the gliadin nanoparticles (Figure 1C).

Characterization of Gliadin-Based Nanoparticles. We measured the size of gliadin or gliadin–gelatin composite nanoparticles using dynamic light scattering (Figure 2, Table 1). At 7% gliadin, the nanoparticles had a uniform size (218.7 ± 5.1 nm average diameter) (Figure 2A) and positive charge (18.5 mV), confirmed by zeta potential analysis. The particles were homogeneous in size and have a narrow distribution. Although gliadin nanoparticles have previously been prepared using emulsification and desolvation techniques,[31,33,35,36,38] their sizes were larger as compared to the electrosprayed gliadin nanoparticles. The gliadin–gelatin composite nanoparticles were created using various ratios of gliadin and gelatin concentrations, such as 7% gliadin/4% gelatin, 7% gliadin/8% gelatin, 14% gliadin/4% gelatin, and 14% gliadin/8% gelatin. The nanoparticles made from 7% gliadin/4% gelatin and 7% gliadin/8% gelatin had an average diameter of 398.6 ± 4.2 nm (Figure 2B) and 450.1 ± 9.7 nm (Figure 2C) with an average zeta potential of 14.2–19 mV. It was observed that the size distribution of 7% gliadin/4% gelatin and 7% gliadin/8% gelatin composite nanoparticles was larger as compared to the 7% gliadin nanoparticles containing homogeneous size distributions. The nanoparticles made from 14% gliadin/8% gelatin did not have a uniform shape and fibrous structures were prominent, suggesting that high concentrations of gliadin and gelatin were not suitable for creating composite nanoparticles (data not shown). In contrast, particles with 7% gliadin/4% gelatin had a uniform shape without fibrous networks (Figure 1B,C). A quantitative analysis of the size distribution demonstrated that the nanoparticle size was directly proportional to the concentrations of gliadin and gelatin polymers. When the gliadin concentration was constant, the particle size increased with the gelatin concentration. The viscosity increased with polymer concentrations, resulting in creating larger particles at higher polymer concentrations.[43,44] Therefore, the optimal concentration of gliadin and gelatin to create uniform nanoparticles was 7% gliadin and 4% gelatin. To confirm whether the gliadin was cross-linked with gelatin in composite nanoparticles, we analyzed the synthesis of composite particles using X-ray diffractometer (Figure 3).

Table 1. Characterization of Gliadin-Based Nanoparticles

number	polymer	average size (nm)	zeta potential (mV)	drug loading (%)
1	7% gliadin	218.66 ± 5.1	18.46 ± 8.3	72.02 ± 5.6
2	7% gliadin/4% gelatin	398.56 ± 4.2	19.00 ± 3.6	64.23 ± 8.9
3	7% gliadin/8% gelatin	450.10 ± 9.7	14.20 ± 3.7	52.77 ± 12.6

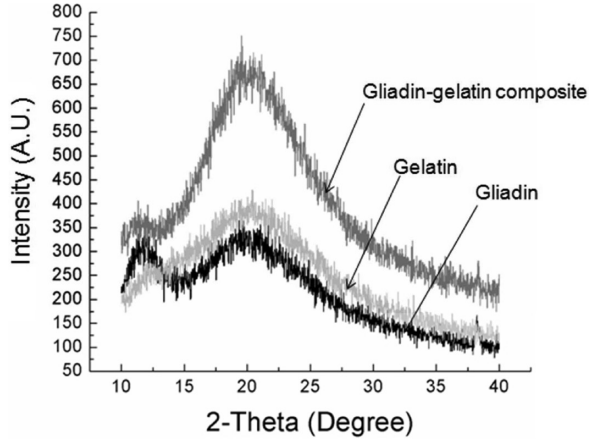

Figure 3. X-ray diffraction pattern of the gliadin–gelatin composite nanoparticle.

Gelatin had a peak at 20°, whereas pure gliadin particles showed two peaks at 12° and 18°. We observed minor and major peaks at 12° and 18–20° in the gliadin–gelatin composite nanoparticles, because the gelatin was bound to the gliadin surface. We also found that gliadin–gelatin composite nanoparticles had higher intensity peaks than gliadin nanoparticles. This result revealed that the gliadin extraction and electrospray deposition process did not change any physical structure of gliadin proteins.

Controlled Drug Release from Gliadin-Based Nanoparticles. Polymeric nanoparticles are of great interest in regulating the delivery and controlled release of drugs. We used cyclophosphamide, an anticancer drug, to confirm the delivery and controlled release from gliadin or gliadin–gelatin composite nanoparticles. Various parameters (e.g., wettability, particle size, degradation rate, molecular weight, and binding affinity between the polymer and drug) play an important role in controlling drug release.[45] Biocompatible polymeric particles could release anticancer drugs in a controlled manner. We quantified the amount of cyclophosphamide released from the nanoparticles using a colorimetric assay and UV–visible

dx.doi.org/10.1021/la300691n | Langmuir 2012, 28, 8216–8223

spectrophotometry. The concentration of released cyclophosphamide could be measured as based on a nitroso derivative of cyclophosphamide. We observed higher percentage of drug loading in gliadin nanoparticles as compared to the gliadin–gelatin composite nanoparticles (Table 1). Higher percentage (72.02%) of drug loading in the gliadin nanoparticles was attributed to the adhesive properties of gliadin polymers as compared to the drug loading efficiency (52.77–64.23%) of gliadin–gelatin composite nanoparticles. We also measured the cyclophosphamide released from nanoparticles synthesized with 7% gliadin, 7% gliadin/4% gelatin, and 7% gliadin/8% gelatin for 48 h (Figure 4). Cyclophosphamide was released from gliadin or gliadin–gelatin composite nanoparticles in two steps. In the first step, cyclophosphamide was rapidly released (46%) from 7% gliadin/8% gelatin composite nanoparticles within 1 h. In contrast, 7% gliadin and 7% gliadin/4% gelatin nanoparticles released 25% and 30% of cyclophosphamide within 1 h, respectively. The rapid release of cyclophosphamide from gliadin or gliadin–gelatin composite nanoparticles might be due to a fraction of the cyclophosphamide adhering to the surface of the nanoparticles[46] or the high aqueous solubility of gelatin.[47] During the initial period of the drug release, the drug on the surface of the nanoparticles reacted with the aqueous medium, resulting in burst release. In the second step, cyclophosphamide was steadily released from the nanoparticles for 48 h. At 48 h, 80%, 90%, and 95% of the cyclophosphamide was released from 7% gliadin, 7% gliadin/4% gelatin, and 7% gliadin/8% gelatin nanoparticles, respectively. The second step was probably due to the drug diffusion from the nanoparticles, as previously described.[48] The rate of drug release was significantly affected by the surface wettability. Composite nanoparticles containing hydrophilic gelatin released drugs in a rapid manner as compared to hydrophobic gliadin nanoparticles. This result suggests that the hydrophobicity of gliadin nanoparticles could manipulate the drug release in a controlled manner.

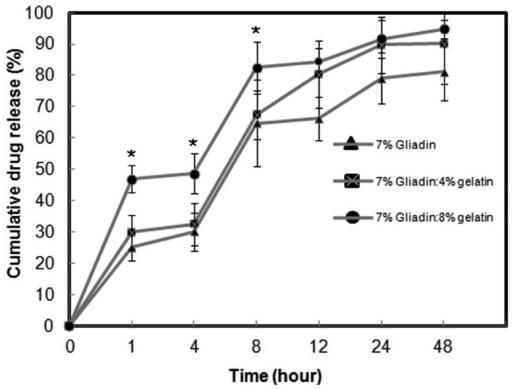

Figure 4. Drug release analysis of cyclophosphamide from gliadin or gliadin–gelatin composite nanoparticles. Data of 7% gliadin/8% gelatin composite nanoparticles were statistically compared to 7% gliadin nanoparticles (*$p < 0.05$).

Apoptosis of Breast Cancer Cells. Natural polymeric nanoparticles have been considered as a safe drug carrier.[19,20] Although gliadin–gelatin composite nanoparticles enabled the release of 89–91% drug at 24 h, we used 7% gliadin nanoparticle (79% release at 24 h) (Figure 4) due to its small size (218.7 nm) and slow release property. We hypothesized that 7% gliadin nanoparticles loaded with cyclophosphamide would induce apoptosis of breast cancer cells. To confirm this hypothesis, we cultured MCF7 breast cancer cells for 24 h with four different experimental conditions. Cells cultured in medium alone (Figure 5A) or with 7% gliadin nanoparticles alone (Figure 5B) did not undergo apoptosis. The breast cancer cells cultured with 7%

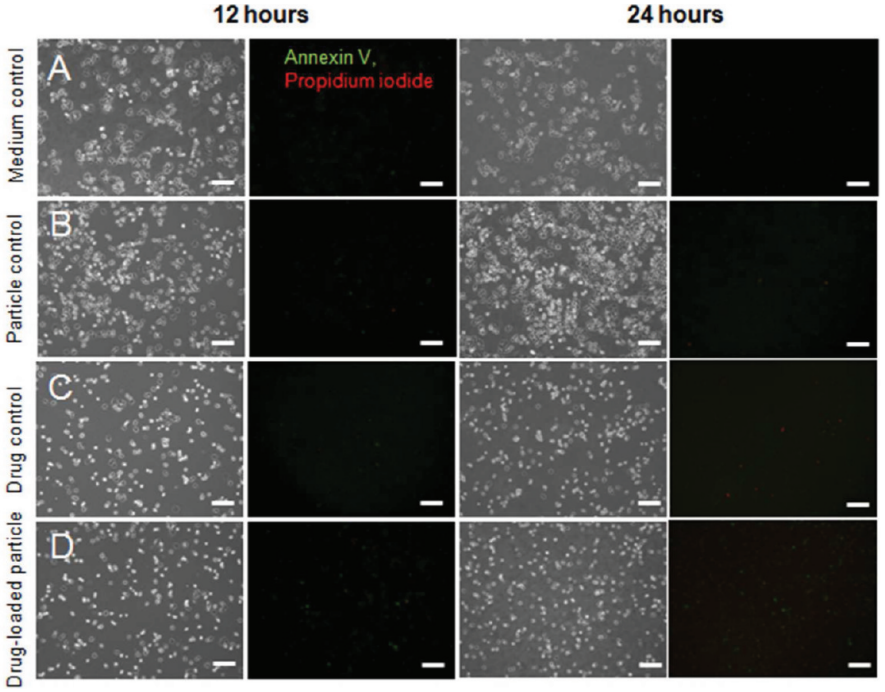

Figure 5. Apoptosis of breast cancer cells cultured with 7% gliadin nanoparticles loaded with cyclophosphamide. The breast cancer cells were cultured with (A) medium alone, (B) 7% gliadin nanoparticles alone, (C) cyclophosphamide alone, and (D) 7% gliadin nanoparticle loaded with cyclophosphamide. Apoptotic and necrotic cells were stained by Annexin V (green) and propidium iodide (red). Scale bars are 300 μm.

dx.doi.org/10.1021/la300691n | *Langmuir* 2012, 28, 8216–8223

gliadin nanoparticles for 24 h remained highly viable, showing that gliadin nanoparticles were biocompatible. When cells were cultured with cyclophosphamide alone for 24 h, some cells were dead (Figure 5C). The cells cultured with 7% gliadin nanoparticles loaded with cyclophosphamide became apoptotic (Figure 5D). However, fluorescent images of the apoptosis assay were not enough evidence to identify whether gliadin nanoparticles loaded with cyclophosphamide could induce apoptosis. Thus, we performed a Western blot analysis to confirm the apoptosis (Figure 6A). We observed that Bcl-2

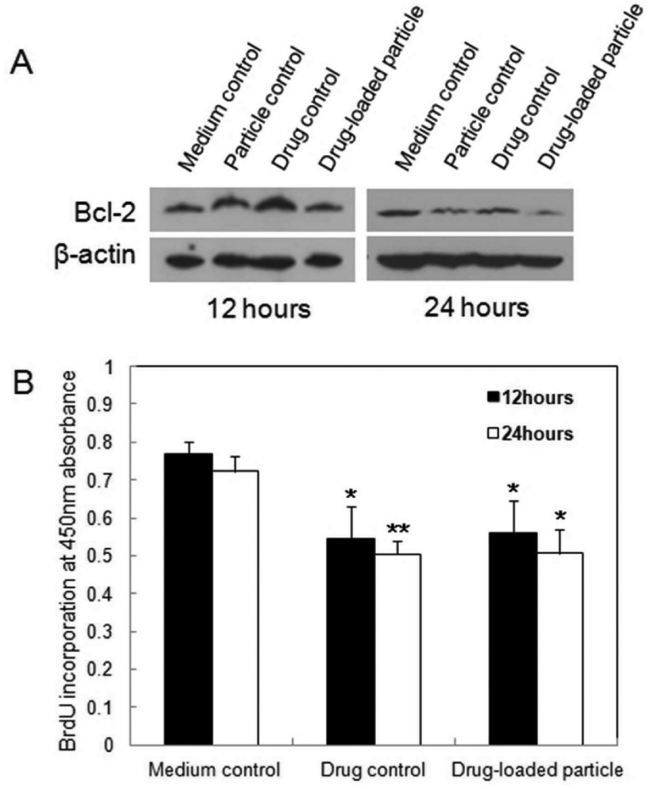

Figure 6. (A) Western blot analysis of breast cancer cells cultured with cyclophosphamide-loaded 7% gliadin nanoparticles, showing that Bcl-2 protein was down-regulated in cells cultured with cyclophosphamide-loaded 7% gliadin nanoparticles for 24 h. (B) BrdU incorporation assay to confirm cell death induced by cyclophosphamide-loaded 7% gliadin nanoparticles. Data from drug control and drug-loaded particles were statistically compared to medium control alone (*$p < 0.05$, **$p < 0.01$).

protein was significantly down-regulated in breast cancer cells cultured with cyclophosphamide-loaded 7% gliadin nanoparticles for 24 h. In contrast, Bcl-2 protein was up-regulated in breast cancer cells cultured with 7% gliadin nanoparticles without cyclophosphamide for 24 h. We also confirmed that cells cultured with cyclophosphamide-loaded gliadin nanoparticles were not apoptotic at 12 h. Interestingly, Bcl-2 was not down-regulated in cells cultured with cyclophosphamide alone for 24 h. To further confirm whether the cyclophosphamide-loaded gliadin nanoparticles induce cell death, we performed the BrdU incorporation assay (Figure 6B). BrdU incorporation assay demonstrated that cyclophosphamide-loaded 7% gliadin nanoparticles induced cell death as compared to medium control alone. This BrdU incorporation assay result corresponded to the data of the apoptosis assay (Figure 5) and Western blotting analysis (Figure 6A), suggesting that cyclophosphamide-loaded 7% gliadin nanoparticles might induce apoptosis. Our result also agreed with the previous work, showing that polymeric particles loaded with cyclophosphamide inhibited tumor growth.[49] Furthermore, our result suggested that gliadin-based nanoparticles might promote the absorption of the anticancer drug due to the bioadhesive property of gliadin. Given its muco/bioadhesive potential, anticancer drug-loaded gliadin nanoparticles might adhere on the surface of cancer cells to induce the apoptosis.

CONCLUSIONS

We synthesized nanoparticles from the natural gliadin polymer using an electrospray deposition system. Gliadin-based nanoparticles enabled the delivery and controlled release of cyclophosphamide anticancer drug in a controlled manner. The size profiles and synthesis of gliadin or gliadin−gelatin composite nanoparticles were characterized by dynamic light scattering and X-ray diffractometry. Although cyclophosphamide was gradually released from gliadin nanoparticles for 48 h, gliadin−gelatin composite nanoparticles released the drug in a rapid manner. Furthermore, breast cancer cells cultured with cyclophosphamide-loaded 7% gliadin nanoparticles for 24 h became apoptotic, confirmed by down-regulation of Bcl-2 protein in Western blot analysis. Therefore, this anticancer drug-loaded gliadin nanoparticle could be a powerful tool for cancer therapy applications.

AUTHOR INFORMATION

Corresponding Author

*E-mail: bchung@hanyang.ac.kr.

Notes

The authors declare no competing financial interest.

ACKNOWLEDGMENTS

This work was supported by the Science Research Program through the National Research Foundation of Korea (NRF) funded by the Ministry of Education, Science and Technology (Grant Number 20110016331, 20110005678, and 2008-0061860). This research was also supported by a grant from the Korea Research Institute of Bioscience and Biotechnology (KRIBB) Initiative Research Program (Grant Number KGM7141111). J. M. Lee and B. Ku were partially supported by Korea Industrial Technology Foundation (KOTEF) through the Human Resource Training Project for Strategic Technology.

REFERENCES

(1) Ashley, C. E.; Carnes, E. C.; Phillips, G. K.; Padilla, D.; Durfee, P. N.; Brown, P. A.; Hanna, T. N.; Liu, J.; Phillips, B.; Carter, M. B.; Carroll, N. J.; Jiang, X.; Dunphy, D. R.; Willman, C. L.; Petsev, D. N.; Evans, D. G.; Parikh, A. N.; Chackerian, B.; Wharton, W.; Peabody, D. S.; Brinker, C. J. The targeted delivery of multicomponent cargos to cancer cells by nanoporous particle-supported lipid bilayers. *Nat. Mater.* **2011**, *10*, 389−397.

(2) Kim, D. K.; Dobson, J. Nanomedicine for targeted drug delivery. *J. Mater. Chem.* **2009**, *19*, 6294−6307.

(3) Lebeau, B.; Chouaïd, C.; Baud, M.; Masanès, M.-J.; Febvre, M. Oral second- and third-line lomustine−etoposide−cyclophosphamide chemotherapy for small cell lung cancer. *Lung Cancer* **2010**, *67*, 188−193.

(4) Kumar, S. K.; Lacy, M. Q.; Hayman, S. R.; Stewart, K.; Buadi, F. K.; Allred, J.; Laumann, K.; Greipp, P. R.; Lust, J. A.; Gertz, M. A.; Zeldenrust, S. R.; Bergsagel, P. L.; Reeder, C. B.; Witzig, T. E.; Fonseca, R.; Russell, S. J.; Mikhael, J. R.; Dingli, D.; Rajkumar, S. V.;

Dispenzieri, A. Lenalidomide, Cyclophosphamide and dexamethasone (CRd) for newly diagnosed multiple myeloma: Results from a phase 2 trial. *Am. J. Hematol.* **2011**, *86*, 640−645.
(5) Russell, H. V.; Groshen, S. G.; Ara, T.; DeClerck, Y. A.; Hawkins, R.; Jackson, H. A.; Daldrup-Link, H. E.; Marachelian, A.; Skerjanec, A.; Park, J. R.; Katzenstein, H.; Matthay, K. K.; Blaney, S. M.; Villablanca, J. G. A phase I study of zoledronic acid and low-dose cyclophosphamide in recurrent/refractory neuroblastoma: A new approaches to neuroblastoma therapy (NANT) study. *Pediatr. Blood Cancer* **2011**, *57*, 275−282.
(6) Davidson, N.; Rapoport, B.; Erikstein, B.; L'Esperance, B.; Ruff, P.; Paska, W.; Miller, I.; Curtis, P. Comparison of an orally disintegrating ondansetron tablet with the conventional ondansetron tablet for cyclophosphamide-induced emesis in cancer patients: A multicenter, double-masked study. *Clin. Ther.* **1999**, *21*, 492−502.
(7) Mukherjee, N.; Delay, E. R. Cyclophosphamide-induced disruption of umami taste functions and taste epithelium. *Neuroscience* **2011**, *192*, 732−745.
(8) Oh, M. S.; Chang, M. S.; Park, W.; Kim, D. R.; Bae, H.; Huh, Y.; Park, S. K. Yukmijihwang-tang protects against cyclophosphamide-induced reproductive toxicity. *Reprod. Toxicol.* **2007**, *24*, 365−370.
(9) Salgueiro, A.; Egea, M. A.; Espina, M.; Valls, O.; García, M. L. Stability and ocular tolerance of cyclophosphamide-loaded nanospheres. *J. Microencapsul.* **2004**, *21*, 213−223.
(10) Salgueiro, A.; Gamisans, F.; Espina, M.; Alcober, X.; García, M. L.; Egea, M. A. Cyclophosphamide-loaded nanospheres: analysis of the matrix structure by thermal and spectroscopic methods. *J. Microencapsul.* **2002**, *19*, 305−310.
(11) Judy, K. D.; Olivi, A.; Buahin, K. G.; Domb, A.; Epstein, J. I.; Colvin, O. M.; Brem, H. Effectiveness of controlled release of a cyclophosphamide derivative with polymers against rat gliomas. *J. Neurosurg.* **1995**, *82*, 481−486.
(12) Gabizon, A. A. Stealth Liposomes and Tumor Targeting: One Step Further in the Quest for the Magic Bullet. *Clin. Cancer Res.* **2001**, *7*, 223−225.
(13) Konishi, M.; Tabata, Y.; Kariya, M.; Suzuki, A.; Mandai, M.; Nanbu, K.; Takakura, K.; Fujii, S. In vivo anti-tumor effect through the controlled release of cisplatin from biodegradable gelatin hydrogel. *J. Controlled Release* **2003**, *92*, 301−313.
(14) Kopeček, J.; Kopečková, P.; Minko, T.; Lu, Z.-R. HPMA copolymer−anticancer drug conjugates: design, activity, and mechanism of action. *J. Pharm. Biopharm.* **2000**, *50*, 61−81.
(15) Kim, J.-H.; Kim, Y.-S.; Park, K.; Lee, S.; Nam, H. Y.; Min, K. H.; Jo, H. G.; Park, J. H.; Choi, K.; Jeong, S. Y.; Park, R.-W.; Kim, I.-S.; Kim, K.; Kwon, I. C. Antitumor efficacy of cisplatin-loaded glycol chitosan nanoparticles in tumor-bearing mice. *J. Controlled Release* **2008**, *127*, 41−49.
(16) Oh, K. S.; Song, J. Y.; Cho, S. H.; Lee, B. S.; Kim, S. Y.; Kim, K.; Jeon, H.; Kwon, I. C.; Yuk, S. H. Paclitaxel-loaded Pluronic nanoparticles formed by a temperature-induced phase transition for cancer therapy. *J. Controlled Release* **2010**, *148*, 344−350.
(17) Elzoghby, A. O.; Abo El-Fotoh, W. S.; Elgindy, N. A. Casein-based formulations as promising controlled release drug delivery systems. *J. Controlled Release* **2011**, *153*, 206−216.
(18) Lu, Y.; Chen, S. C. Micro and nano-fabrication of biodegradable polymers for drug delivery. *Adv. Drug Delivery Rev.* **2004**, *56*, 1621−1633.
(19) Lin, W.; Coombes, A. G. A.; Garnett, M. C.; Davies, M. C.; Schacht, E.; Davis, S. S.; Illum, L. Preparation of sterically stabilized human serum albumin nanospheres using a novel dextranox-MPEG crosslinking agent. *Pharm. Res.* **1994**, *11*, 1588−1592.
(20) Coester, C.; Nayyar, P.; Samuel, J. In vitro uptake of gelatin nanoparticles by murine dendritic cells and their intracellular localisation. *J. Pharm. Biopharm.* **2006**, *62*, 306−314.
(21) Gulfam, M.; Lee, J. M.; Chung, B. G. Two-phase bioreactor system for cell-laden hydrogel assembly. *Biotechnol. Prog.* **2011**, *27*, 466−472.
(22) Hoare, T. R.; Kohane, D. S. Hydrogels in drug delivery: Progress and challenges. *Polymer* **2008**, *49*, 1993−2007.
(23) Hamidi, M.; Azadi, A.; Rafiei, P. Hydrogel nanoparticles in drug delivery. *Adv. Drug Delivery Rev.* **2008**, *60*, 1638−1649.
(24) Lai, J.-Y. Biocompatibility of chemically cross-linked gelatin hydrogels for ophthalmic use. *J. Mater. Sci. Mater. Med.* **2010**, *21*, 1899−1911.
(25) Baino, F. Towards an ideal biomaterial for vitreous replacement: Historical overview and future trends. *Acta Biomater.* **2011**, *7*, 921−935.
(26) Dreesmann, L.; Ahlers, M.; Schlosshauer, B. The pro-angiogenic characteristics of a cross-linked gelatin matrix. *Biomaterials* **2007**, *28*, 5536−5543.
(27) Zhang, T.; Yan, Y.; Wang, X.; Xiong, Z.; Lin, F.; Wu, R.; Zhang, R. Three-dimensional gelatin and gelatin/hyaluronan hydrogel structures for traumatic brain injury. *J. Bioact. Compat. Polym.* **2007**, *22*, 19−29.
(28) Wang, X.; Yu, X.; Yan, Y.; Zhang, R. Liver tissue responses to gelatin and gelatin/chitosan gels. *J. Biomed. Mater. Res., Part A* **2008**, *87*, 62−68.
(29) Umamaheshwari, R. B.; Ramteke, S.; Jain, N. K. Anti-*Helicobacter pylori* effect of mucoadhesive nanoparticles bearing amoxicillin in experimental gerbils model. *AAPS PharmSciTech* **2004**, *5*, 60−68.
(30) Gurny, R.; Meyer, J.-M.; Peppas, N. A. Bioadhesive intraoral release systems: design, testing and analysis. *Biomaterials* **1984**, *5*, 336−340.
(31) Ezpeleta, I.; Arangoa, M. A.; Irache, J. M.; Stainmesse, S.; Chabenat, C.; Popineau, Y.; Orecchioni, A.-M. Preparation of Ulex europaeus lectin-gliadin nanoparticle conjugates and their interaction with gastrointestinal mucus. *Int. J. Pharm.* **1999**, *191*, 25−32.
(32) Arangoa, M. A.; Campanero, M. A.; Renedo, M. J.; Ponchel, G.; Irache, J. M. Gliadin nanoparticles as carriers for the oral administration of lipophilic drugs. Relationships between bioadhesion and pharmacokinetics. *Pharm. Res.* **2001**, *18*, 1521−1527.
(33) Duclairoir, C.; Orecchioni, A. M.; Depraetere, P.; Osterstock, F.; Nakache, E. Evaluation of gliadins nanoparticles as drug delivery systems: a study of three different drugs. *Int. J. Pharm.* **2003**, *253*, 133−144.
(34) Aguzzi, A. Unraveling prion strains with cell biology and organic chemistry. *Proc. Natl. Acad. Sci. U.S.A.* **2008**, *105*, 11−12.
(35) Ezpeleta, I.; Irache, J. M.; Stainmesse, S.; Chabenat, C.; Gueguen, J.; Popineau, Y.; Orecchioni, A.-M. Gliadin nanoparticles for the controlled release of all-trans-retinoic acid. *Int. J. Pharm.* **1996**, *131*, 191−200.
(36) Zhang, X.; Do, M. D.; Dean, K.; Hoobin, P.; Burgar, I. M. Wheat-gluten-based natural polymer nanoparticle composites. *Biomacromolecules* **2007**, *8*, 345−353.
(37) Jahanshahi, M.; Sanati, M. H.; Babaei, Z. Optimization of parameters for the fabrication of gelatin nanoparticles by the Taguchi robust design method. *J. Appl. Stat.* **2008**, *35*, 1345−1353.
(38) Duclairoir, C.; Nakache, E.; Marchais, H.; Orecchioni, A. M. Formation of gliadin nanoparticles: Influence of the solubility parameter of the protein solvent. *Colloid Polym. Sci.* **1998**, *276*, 321−327.
(39) Xie, J.; Marijnissen, J. C. M.; Wang, C.-H. Microparticles developed by electrohydrodynamic atomization for the local delivery of anticancer drug to treat C6 glioma in vitro. *Biomaterials* **2006**, *27*, 3321−3332.
(40) Bohr, A.; Kristensen, J.; Stride, E.; Dyas, M.; Edirisinghe, M. Preparation of microspheres containing low solubility drug compound by electrohydrodynamic spraying. *Int. J. Pharm.* **2011**, *412*, 59−67.
(41) Gulfam, M.; Lee, J. M.; Kim, J.-e.; Lim, D. W.; Lee, E. K.; Chung, B. G. Highly porous core−shell polymeric fiber network. *Langmuir* **2011**, *27*, 10993−10999.
(42) Jaworek, A.; Sobczyk, A. T. Electrospraying route to nanotechnology: An overview. *J. Electrostat.* **2008**, *66*, 197−219.
(43) Zhang, S.; Kawakami, K. One-step preparation of chitosan solid nanoparticles by electrospray deposition. *Int. J. Pharm.* **2010**, *397*, 211−217.

(44) Hartman, R. P. A.; Brunner, D. J.; Camelot, D. M. A.; Marijnissen, J. C. M.; Scarlett, B. Jet break-up in electrohydrodynamic atomization in the cone-jet mode. *J. Aerosol Sci.* **2000**, *31*, 65−95.
(45) Ge, H.; Hu, Y.; Jiang, X.; Cheng, D.; Yuan, Y.; Bi, H.; Yang, C. Preparation, characterization, and drug release behaviors of drug nimodipine-loaded poly(epsilon-caprolactone)-poly(ethylene oxide)-poly(epsilon-caprolactone) amphiphilic triblock copolymer micelles. *J. Pharm. Sci.* **2002**, *91*, 1463−1473.
(46) Vassiliou, A. A.; Papadimitriou, S. A.; Bikiaris, D. N.; Mattheolabakis, G.; Avgoustakis, K. Facile synthesis of polyester-PEG triblock copolymers and preparation of amphiphilic nanoparticles as drug carriers. *J. Controlled Release* **2010**, *148*, 388−395.
(47) Zhang, L.; Hu, Y.; Jiang, X.; Yang, C.; Lu, W.; Yang, Y. H. Camptothecin derivative-loaded poly(caprolactone-co-lactide)-b-PEG-b-poly(caprolactone-co-lactide) nanoparticles and their biodistribution in mice. *J. Controlled Release* **2004**, *96*, 135−148.
(48) Duclairoir, C.; Orecchioni, A. M.; Depraetere, P.; Nakache, E. α-Tocopherol encapsulation and in vitro release from wheat gliadin nanoparticles. *J. Microencapsul.* **2002**, *19*, 53−60.
(49) Yaeger, K. A.; Kurt, R. A. Construction and evaluation of a combined cyclophosphamide/nanoparticle anticancer vaccine. *J. Cancer Ther.* **2011**, *2*, 384−393.